2 (mix)

Page One Title

PHASE-BOUNDARY IMPEDANCE OF NOBLE-METAL ELECTRODES IN THE REGION OF HYDROGEN ADSORPTION I. ACTIVATED PLATINUM ELECTRODES

M. Breiter, H. Kammermaier, and C. A. Knorr

Translation of "Untersuchung der Phasengrenzimpedanz an Edelmetallelektroden im Gebiet der Wasserstoffadsorption," Zeitschrift fuer Elektrochemie, Vol. 60, No. 1, 1956, pp. 37-47

(4")

NATIONAL AERONAUTICS AND SPACE ADMINISTRATION
WASHINGTON, D.C. NASA AUGUST 1972

25

NASA TT F-14,365

PHASE-BOUNDARY IMPEDANCE OF NOBLE-METAL ELECTRODES IN THE REGION OF HYDORGEN ADSORPTION
I. ACTIVATED PLATINUM ELECTRODES

Cover Page Title

M. Breiter, H. Kammermaier, and C. A. Knorr

ABSTRACT: With a special system of measuring electrodes the authors investigate hydrogen adsorption on platinum electrodes. Comparisons using direct and alternating currents, high and low voltages, and various ranges are both described and charted for atomic and molecular hydrogen with the almost always linear proportions of the functions provided.

Cover Page Source

INTRODUCTION

Tests on smooth platinum electrodes in 8n-H_2SO_4 with H_2 rinsing are discribed. In order to be able to compare successively determined measuring values with each other, it has proven to be necessary to activate the electrodes by anodic current impulses between every measurement. This treatment makes it possible to obtain a high activity surface condition on the platinum which can be uniformly reproduced. Without these measurements there are generally at first temperal changes in the activity which only lead to a uniformly constant final position of rather low activity after a rather long period of time, but which is only conditionally reproducible. The frequency and potential dependency of the alternating current resistance of the activated platinum electrodes can be discribed quantitatively to a large extent in all of the over voltage ranges investigated, with consideration given only to the adsorption of the H atoms, the diffusion of the H_2 molecules and the discharge of the H^+ ions.

/37*

1. Test Methodology

Figure 1 diagrams the alternating current and the direct current circuit of the measurement apparatus. The variable frequency alternating current, produced with a RC Generator from the Rohde and Schwarz Company, is divided into two parallel branches one of which contains the test cell (between E and G) and the

NASA

*Numbers in the margin indicate pagination in the foreign text.

other a measurement resistance (between D and G) adjustable from 0.1Ω to 11kΩ. The measurement of the absolute amount (R) of the electrode impedance takes place in such a way that first the alternating volatage U_{FG} between the pick-up and the grounded test electrodes was given on a high ohm (initial resistance 1MΩ) alternating current tube volt meter of the Philips Company and adjusted by varying the initial generator voltage at 5mV. Then, without changing the initial voltage of the generator, the same alternating voltage was picked up with a variable measurement (DG) through which the same alternating flows as through the test cell, because of the uniformity of the very great barrier resistance (A-B and A-C) and capacitors (B-D and C-E) of the relative magnitude and phase relationship. The value of the measurement resistance adjusted in this way was then equal to the absolute amount of impedance, which could be exactly determined at about 2% in this way.

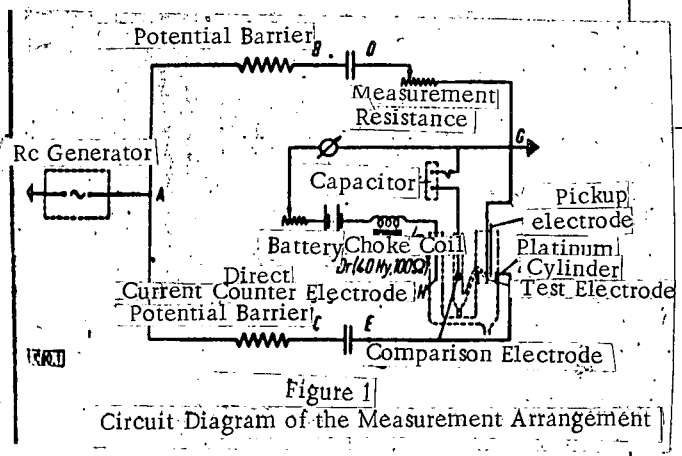

Figure 1
Circuit Diagram of the Measurement Arrangement

Determination of the phase angle φ of the direct current resistance was achieved by using a homemade measuring apparatus [1]. In it, according to a principle originating with Opitz [2,3], two out of phase alternating voltages of the same magnitude are increased independently of each other and of the phase about 200 times at the test electrode and at the measurement resistance, and then turned into square waves of a constant magnitude. Producing the square waves, which occurs with the Opitz process quite simply with heavy overloading of suitable triodes, is achieved here by means of two amplitude discriminators according to the "Schmitt-Trigger" circuit [4]. The use of this so called flip-flop circuit has the advantage on the one hand that with two potentiometers the square waves corresponding to the two alternating voltages can always be adjusted exactly to the same length and, on the other hand, the impulses have a very good transition length (10^{-7} sec). The two square waves, which are mutually out of

phase by the same angle φ as their pertinent alternating voltages, are now superimposed upon one another with the aid of a backlash circuit consisting of germanium diodes in such a way that a constant direct current is produced only during the time that they do not overlap. Thus the mean value in time of the rectified current denoted by a galvanometer is proportional to the phase displacement φ which confirms the assembly calibration undertaken repeatedly with the help of RC members with suitable dimensions. Before the measurements the same alternating voltage was always applied to the two imputs of the phase meter and the phase displacement 0 current indicated by the apparatus was always set at a minimum by means of the two mentioned potentiometers in order to guarantee the specified uniformity of the two square waves. In addition the exact correspondence of reading of the 90° phase displacement with the calibration was checked repeatedly with the help of static capacitors with a very small loss angle which could be connected to the alternating current circuit as objects of measurement instead of the test cell. In this way the phase displacement φ could be exactly determined in the frequency range 30 Hz to 20kHz with uniform sensitivity over the angel spread form 0 to 90° within 1°. (4'') /38

The way of producing the direct current pre-polarization was different depending upon whether the tests were carried out with negative or positive overload. The direct current circuit shown in Figure 1, which was separated from the adequatly large choke coil Dr from the alternating current circuit, was used in the research in the area of cathodic overload. A stationary potential was induced on the electrode by a constant direct current whose magnitude could be regulated by an adjustable potential barrier. In order to eliminate the depolarizing effect of the anodically developed oxygen on the test electrode, the direct current was conducted through the counterelectrode H, found in another part of the vessel. However, this method of producing the direct current polarization could not be used in the region of the H_2 diffusion limiting current, since the potential here is subject to large punctuations with a strong current, as is well known. Therefore the direct current pre-polarization was set up in the positive overload area andthe tests by means of a low resistance potentiometer circuit to force the potential constantly upon the electrode instead of the current. In order to avoid a noticable voltage drop, the platinum plated platinum cylinder

conveying the alternating current, set for 0 potential with the H_2 rinsing applied, was used here as a counterelectrode. Measurement of the limiting current took place by determining the voltage drop at the choke coil, which in this case was connected from the platinum cylinder.

In the test vessel [5] was found the grounded test electrode in a field cylindrically symmetrical with respect to the alternating current. In order to keep edge disturbances in the field as small as possible, a glass bead was soldered at one end of the electrode and on the other side the electrolyte was added to exactly the height of the electrode. The electrolyte resistance between the test electrode and the platinum plated pick-up load submerged in the vicinity, including the conductor resistances present, was determined at very high frequencies (150-300 kHz) by measuring the absolute amount of the alternating current resistance, which becomes practically independent of frequency here. In the measurement discribed below the electrolyte resistance determined in this way was always deducted from the resistance component of the alternating current resistance in series.

(4")

A platinum plated platinum plate, rinsed with molecular hydrogen, was used as the test electrode I (cf. Figure 1) to measure the over voltage . The part of the vessel containing the comparison electrode was connected with the part containing the test electrode through a capillary ending in its vacinity.

The entire vessel was sealed against outer air by a simple construction in valves as well as by an overflow reservior.

2. Theoretical Considerations

First the frequency and potential dependence of both components of the alternating current resistance is derived for the entire over voltage area under study. If the small perodic changes in the different magnitudes caused by the sinusoidal alternating current are designated by Δ, and if the effect of molecular hydrogen adsorbed on the electrode surface is also considered, the following

edge condition will exist on the electrode surface (at a distance x = 0)[1]:

$$-F\frac{d\Delta c_H}{dt} - 2F\frac{d\Delta_a c_{H_2}}{dt} = \Delta i_F - 2DF\left(\frac{\partial \Delta c_{H_2}}{\partial x}\right)_{x=0} \quad (1)$$

The well known diffusion equation is valid for the molecular hydrogen in the electrolyte in the immediate vacinity.

$$\frac{\partial \Delta c_{H_2}}{\partial t} = D \cdot \frac{\partial^2 \Delta c_{H_2}}{\partial x^2} \quad (2)$$

c_H Surface concentrationof the adsorbed atomic hydrogen in g eq-cm^2

$a c_{H_2}$ Surface concentration of the adsorbed molecular hydrogen in Mol/cm^2

c_{H_2} Volume concentration of the molecular hydrogen in Mol/cm^3

D- Diffusion coefficient of the molecular hydrogen in the electrolyte in cm^2/sec

(4'')

F Farday Constant in Coul/Mol

$i_F(\eta, c_H)$ Faraday current which depends explicitly upon η and c_H

A very large part of the test results on active smooth platinum electrodes can be very well discribed quantitatively, as can be seen individually in the experiments referring to the frequency and potential dependency in the entire overload area, if the following simplifications are accepted:

a) The H_2 combining equilibrium is standardized

$$\Delta_a c_{H_2} = \frac{d_a c_{H_2}}{d c_H} \cdot \Delta c_H \quad (3a)$$

[1] It is simply presumed in equation (1) that the absorption of the H atoms and H_2 molecules in respect to the currents causing them is displaced exactly 90° in phase.

b) The equilibrium is standardized between the molecular hydrogen on the electrode and in the electrolyte

Page One Title

$$\Delta_a c_{H_2} = \frac{d_a c_{H_2}}{d c_{H_2}} \cdot \Delta c_{H_2}. \tag{3b}$$

Below we presume that $(d_a c_{H_2})/dc_{H_2} = k$ = constant, especially if the heat of adsorption of the molecular hydorgen is relatively small[2].

With assumption a) equation (1) first transformed into

$$-F\left(1 + 2\frac{d_a c_{H_2}}{d c_H}\right)\frac{d\Delta c_H}{dt} = \Delta i_F - 2FD\left(\frac{\partial \Delta c_{H_2}}{\partial x}\right)_{x\,=\,0} \tag{4}$$

If we with Grahame[7]:

$$\Delta i_F = \frac{\partial i_F}{\partial \eta} \cdot \Delta \eta + \frac{\partial i_F}{\partial c_H} \cdot \Delta c_H. \tag{5}$$

consideration of assumption b) according to the usual methods [7,8] of calculating the alternating current resistance R gives us: /39

$$\Re = \frac{\partial \eta}{\partial i_F} + \frac{\partial \eta}{\partial i_F}\cdot\frac{\partial i_F}{\partial c_H}\cdot\frac{1}{j\omega F\left(1 + 2k\frac{d c_{H_2}}{d c_H}\right) + (1+j)F\frac{d c_{H_2}}{d c_H}\cdot\sqrt{2D\omega}} \tag{6}$$

ω = Circuit frequency of the alternating current

$j = \sqrt{-1}$.

If the discharge equilibrium is standardized ($\eta = \eta_k$) in the direct flux, which may be presumed in our tests, equation (6) can be transformed, with consideration of equation (5) and the Nernst equation form molecular hydrogen, into:

$$\Re = \frac{\partial \eta}{\partial i} + \frac{1}{-j\omega F\left(1 + 2k\frac{d c_{H_2}}{d c_H}\right)\frac{d c_H}{d \eta_K} + \frac{2F^2 c_{H_2}}{RT}(1+j)\sqrt{2D\omega}}. \tag{7}$$

[2] See [6]; in agreement concerning the heat of adsorption of a H_2 molecule at about 0.1 cV and 2 H atoms at 4.55 cV.

With the designations

$$r = \left(\frac{\partial \eta}{\partial i}\right) \qquad (8)$$

$$C_s = -F\left(1 + 2k\frac{dc_{H_2}}{dc_H}\right)\cdot\frac{dc_H}{d\eta_K} = -F\left(\frac{dc_H}{d\eta_K} + 2k\frac{dc_{H_2}}{d\eta_K}\right) \qquad (9)$$

equation (7) is finally written as

$$\Re = r + \frac{1}{j\omega C_s + \frac{2F^2\cdot c_{H_2}}{RT}(1+j)\sqrt{2D\omega}}. \qquad (10)$$

A circuit diagram equivalent to equation (10) for R is diagramed in Figure 2. C_2, corresponding here to the assumption [6] introduced with equation (1), is understood here as a loss free adsorption capacity. If equation (10) is calculated in parallel, consideration of the double layer capacity C_D lying parallel to R leads to:

$$C_p = C_D + \frac{C_s + \frac{2F^2\cdot c_{H_2}}{RT}\sqrt{\frac{2D}{\omega}}}{\left(1 + r\frac{2F^2\cdot c_{H_2}}{RT}\sqrt{2D\omega}\right)^2 + r^2\left(\omega C_s + \frac{2F^2\cdot c_{H_2}}{RT}\sqrt{2D\omega}\right)^2} \qquad (11)$$

$$\frac{1}{R_p} = \frac{\frac{2F^2\cdot c_{H_2}}{RT}\sqrt{2D\omega}\left(1 + r\frac{2F^2\cdot c_{H_2}}{RT}\sqrt{2D\omega}\right) + r\left(\omega C_s + \frac{2F^2\cdot c_{H_2}}{RT}\sqrt{2D\omega}\right)^2}{\left(1 + r\frac{2F^2\cdot c_{H_2}}{RT}\sqrt{2D\omega}\right)^2 + r^2\left(\omega C_s + \frac{2F^2\cdot c_{H_2}}{RT}\sqrt{2D\omega}\right)^2}. \qquad (12)$$

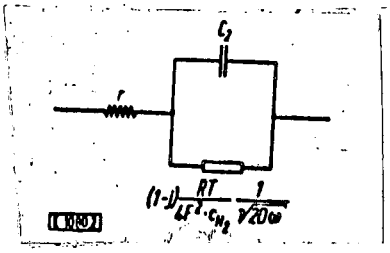

Figure 2. Equivalent Circuit Diagram for R According to Equation (10).

For small frequencies the Warburg [9,10] formulae are derived from equations (10,11,12) where C_D is also naturally taken into consideration:

$$C_p = C_D + C_s + \frac{2F^2\cdot c_{H_2}}{RT}\sqrt{\frac{2D}{\omega}} \qquad (13)$$

$$R_p = \frac{RT}{2F^2\cdot c_{H_2}}\cdot\frac{1}{\sqrt{2D\omega}}. \qquad (14)$$

If C_p is ploted against $(1)/\gamma\omega$ the slop of the straight line part of the curve for small frequencies is proportional to c_{H_2}. The value of $C_2 + C_D$ is found according to equation (13) from the ordinate section of the straight part of the C_p - $(1)/\sqrt{\omega}$ curve obtained by extrapolating to the frequency < infinity.

If c_{H_2} is practically equal to 0, which is the case when active platinum electrode in the potential range $\eta > +50$ MV, we simply read expressions (11,12) in the following way:

$$C_p = C_D + \frac{C_0}{1 + \omega^2 r^2 C_0^2} \tag{15}$$

$$\frac{1}{R_p} = \frac{\omega^2 r C_0^2}{1 + \omega^2 r^2 C_0^2}. \tag{16}$$

These formulae have already been derived with special assumptions by Dolin and Ershler [11] for the positive over voltage area.

3. Tests on Active Platinum Electrodes

We shall first discuss the measurements of the alternating current resistance of smooth, active platinum electrodes with positive over voltage ($\eta > 0$). The electrode was constantly rinsed with molecular hydrogen and the corresponding over voltage instituted by applying a definate voltage across the total cell in the manner described in section 1. Figure 3 gives the plot of the capacity C_p calculated for the parallel circuit and Fibure 3b gives the plot of the resistance conductivity $(1)/R_p$ of the pertinent platinum electrode with a geometrical surface of 0.069cm^2 for various frequencies against the potential. The C_p - η curves, particularly with frequencies $\nu \leq 1.7$ kHz, show a characteristic slope /40 with two clearly marked maxama at η = +100mV and +200 mV in a medium frequency range, as do the $(1)/R_p$ - η curves. Similar results were obtained earlier by Dolan and Ershler [11] (although the maximum η = +200mV) and by Eucken and Weblus [12,13]. Along with the impedance measurements mentioned, the pertinent voltage was likewise determined in all cases (4). This, as always, constantly showed an anodic limiting current on active platinum electrodes which amounted in the present case from η = +50mV to 730 (μA)/cm^2 and was at least mainly determined by the stream of molecular hydrogen to the electrode [14].

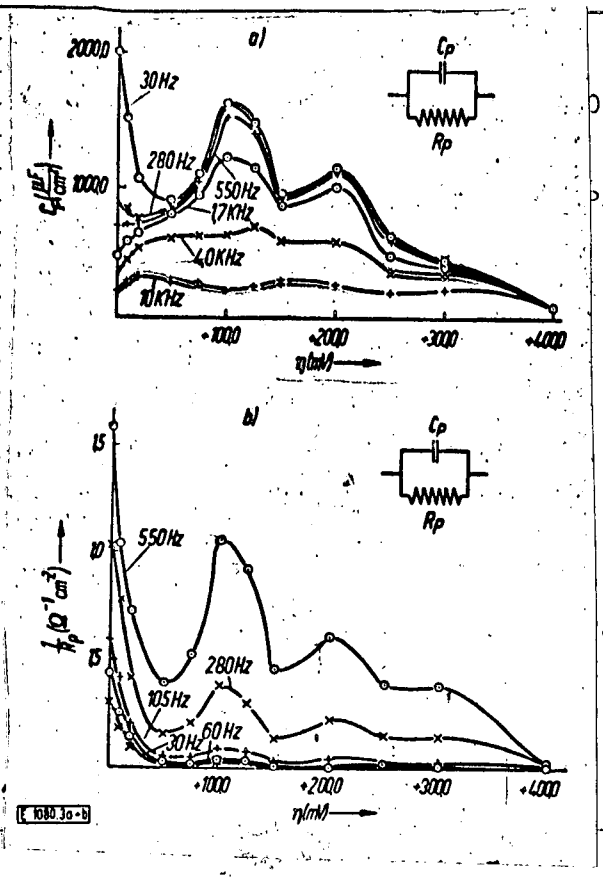

Figure 3. a, Dependence of capacity C_p for various frequencies on overvoltage η in the positive area $\eta > 0$; b, Dependence of the resistant conductivity (1) R_p for various frequencies on the overvoltage η in the potential range $\eta > 0$.

The increase in the curves of C_p - η and (1)/R_p - η, especially for frequencies ν = 550Hz, with a dropping over voltage in the potential range $0 \leqslant \eta \leqslant +50$mV has already been explained by Dolan and Ersher as well as by Eucken and Weblus has caused by the influence of molecular hydrogen on the alternating current resistance. The voltage curve in Figure 4 also shows that the concentration of the molecular hydrogen on the electrode from η = +50mV continually increases from the zero value. The part of the C_p - η curve for $\eta \geqslant +50$mV is, in agreement with the explanation of authors mentioned, to be attributed to the influence of the atomic hydrogen adsorbed onto the surface. In the region of the capacity minimum the effects of the molecular and atomic hydrogen overlap. As can be seen from Figure 3a, the C_p minimum for small frequencies lies at a potential of about +50mV and, as is understandable, shifts to more negative over voltage levels with increasing frequency.

The frequency dependents of both resistance components measured in the potential area $+400\text{mV} \geqslant \eta \geqslant +50\text{mV}$ is presented in Figure 5a (C_p against $1/\sqrt{\omega}$ and 5b ((1)/R_p against ν). The C_p - $1/\sqrt{\omega}$ curves tend for small frequency

toward a limiting value which depends upon the potential (Figure 3a) and essentialy corresponds to the pseudo capacity of the adsorbed hydrogen. This limiting value becomes constantly smaller from η = +250mV with increasing over voltage. When η = +400mV, C_p(30Hz) is finally only slightly different from C_p(10 kHz) [15]. As Voelkl [17,18,19,20] also found, the fact is that at this potential the hydrogen covering of the surface of the active platinum electrodes is practically equal to zero, so that we already find ourselves in the double layer region. /41

As is known, even in the double layer region the electrode does not behave as a pure capacitor of capacity C_D, which is shown by the presence of a small resistant component $(1)/R_{pD}$ (Figure 5b). For high frequencies the $(1)/R_p$ - ν curves approach a limiting value which is almost reached at 20kHz and is still involed in their potential dependence. A frequency dependence of this type on $(1)/R_p$ was first noticed on smooth platinum electrodes by Dolan and Ersher [11], who assigned the limiting value to a reciprocal discharge resistance $(1)/r$.

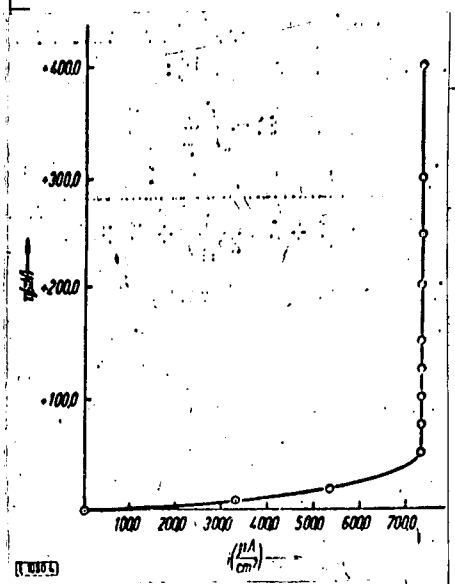

Figure 4. Current Voltage Curve in the Area of the Anodic Diffusion Limiting Current.

The experimental C_p values with three over voltages (+50mV, +150mV, +250mV) calculated according to equation (15) are compared in Table 1. Here the experimental value of 73μF/dm^2 (cf. Figure 3a) was used for C_D and a value determined according to the formula

$$\frac{1}{r} = \frac{1}{R_p(\eta, 20\,\text{kHz})} - \frac{1}{R_p(+400\,\text{mV}, 20\,\text{kHz})} \qquad (17)$$

was used for r.[3] The correction made in this way to $(1)/R_p(\eta, 20\text{kHz})$ comes to a maximum of about 10% because of the resistance component of the double layer impedance (at η = +250mV). Table 1 shows between experiment and theory a very good agreement which Dolan and Ersher were not yet able to obtain in their measurements. Just as with our tests on iridium

[3] We are grateful to Dr. H. Gerischer for a reference to this.

electrodes, their results did not reach any limiting value of C_p for low frequencies. The deviations between the theoretical and experiment values were explained by Dolan and Ersher with the restricted surface diffusion of atomic hydrogen.

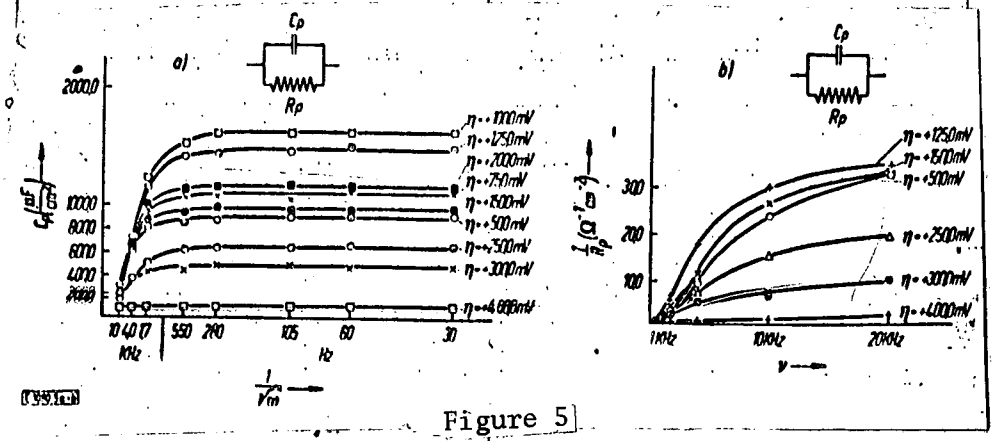

Figure 5

Cover Page Source

a) Frequency Dependence on C_p at Various Over Voltages in the Potential Area +50 mV $\leqslant \eta \leqslant$ + 400mV.

b) Frequency Dependence on (1)/R_p at Various Over Voltages in the Potential Area +50 mV $\leqslant \eta \leqslant$ + 400mV.

(4")

TABLE 1: COMPARISON OF THE C_p VALUES CALCULATED ACCORDING TO EQUATION (15) WITH THE VALUES MEASURED AT OVERVOLTAGES OF +50mV + 150mV and + 250mV

η / C_s / r / ν (Hz)	+ 50 mV 826 μF/cm² 0,0324 $\Omega \cdot$ cm²		+ 150 mV 890 μF/cm² 0,0324 $\Omega \cdot$ cm²		+ 250 mV 572 μF/cm² 0,0575 $\Omega \cdot$ cm²	
	C_p Calculated	C_p Measured	C_p Calculated	C_p Measured	C_p Calculated	C_p Measured
10000	289 μF/cm²	304 μF/cm²	280 μF/cm²	294 μF/cm²	183 μF/cm²	193 μF/cm²
4000	640 μF/cm²	630 μF/cm²	655 μF/cm²	615 μF/cm²	415 μF/cm²	370 μF/cm²
1700	835 μF/cm²	810 μF/cm²	885 μF/cm²	870 μF/cm²	580 μF/cm²	506 μF/cm²
550	891 μF/cm²	850 μF/cm²	952 μF/cm²	939 μF/cm²	638 μF/cm²	608 μF/cm²
280	895 μF/cm²	863 μF/cm²	960 μF/cm²	973 μF/cm²	642 μF/cm²	639 μF/cm²
105	899 μF/cm²	895 μF/cm²	965 μF/cm²	961 μF/cm²	645 μF/cm²	635 μF/cm²
60	899 μF/cm²	897 μF/cm²	965 μF/cm²	954 μF/cm²	645 μF/cm²	652 μF/cm²
30	899 μF/cm²	899 μF/cm²	965 μF/cm²	970 μF/cm²	645 μF/cm²	646 μF/cm²

The corresponding investigation of the frequency dependents of R_p according to equation (16), with the same over voltage values, is illustrated in Table 2. This shows that equation (16) satisfactorily describes the experimental result for high frequencies, while considerable deviations occur for low frequencies.

Although the resistance component in this potential range forms only a small part of the alternating resistance and therefore the R_p values must be accepted with significant measuring errors, the deviations are quite far from the limit of error. The reason for this is presumed to be that the adsorption capacity, as assumed in the theory of equation (1), is not completely loss free. We intend to make a closer investigation of this finding. The potential dependence of $(1)/R_p$, which should be similar to that of C_n according to equation (16) with frequencies which are not too high, demonstrates this behavior only in a central frequency range for the same reason. /42

TABLE 2: COMPARISON OF THE R_p VALUES CALCULATED ACCORDING TO EQUATION (16) WITH THOSE MEASURED AT OVER VOLTAGES OF +50mV, +150 mV and +250mV

η	+ 50 mV		+ 150 mV		+ 250 mV	
ν (Hz)	R_p Calculated	R_p Measured	R_p Calculated	R_p Measured	R_p Calculated	R_p Measured
10000	0,0438 Ω·cm²	0,0414 Ω·cm²	0,0421 Ω·cm²	0,0382 Ω·cm²	0,0705 Ω·cm²	0,067 Ω·cm²
4000	0,104 Ω·cm²	0,104 Ω·cm²	0,0938 Ω·cm²	0,085 Ω·cm²	0,141 Ω·cm²	0,133 Ω·cm²
1700	0,428 Ω·cm²	0,372 Ω·cm²	0,370 Ω·cm²	0,276 Ω·cm²	0,525 Ω·cm²	0,412 Ω·cm²
550	3,80 Ω·cm²	2,53 Ω·cm²	3,82 Ω·cm²	2,15 Ω·cm²	4,60 Ω·cm²	2,57 Ω·cm²
280	14,8 Ω·cm²	6,28 Ω·cm²	12,5 Ω·cm²	7,50 Ω·cm²	17,3 Ω·cm²	6,62 Ω·cm²
105	104 Ω·cm²	17,0 Ω·cm²	89,0 Ω·cm²	33,0 Ω·cm²	123 Ω·cm²	27,5 Ω·cm²
60	318 Ω·cm²	33,8 Ω·cm²	273 Ω·cm²	101 Ω·cm²	380 Ω·cm²	49,5 Ω·cm²
30	1270 Ω·cm²	48,8 Ω·cm²	1090 Ω·cm²	112 Ω·cm²	1500 Ω·cm²	96,5 Ω·cm²

Before more conclusions about the coating of the electrode with hydrogen are discussed for the potential dependence of C_2, the frequency dependence of C_p and R_p in the potential range $0 \leqslant \eta \leqslant +50$mV should be discussed. In Figures 6a and 6b C_p and R_p are presented for some over voltages against $1/\sqrt{\omega}$. For rather small frequencies the curves show the characteristic straight line slopes for the H_2 molecule diffusion, as is to be expected from equations (13,14). While the rise in R_p - $(1)/\gamma\omega$ curves constantly increases with an increasing positive over voltage because of the dropping H_2 concentration on the electrode, the downward slope of the linear part of the C_2 $1/\sqrt{\omega}$ curves drops inversely, to almost completely disappear finally for η = +50mV. Extrapolation of the straight part of the C_p - $(1)/\gamma\omega$ curves to a frequency ∞ infinity, in agreement with equation (13), leads to the value $C_2 + C_D$ as the ordinate section.

NASA

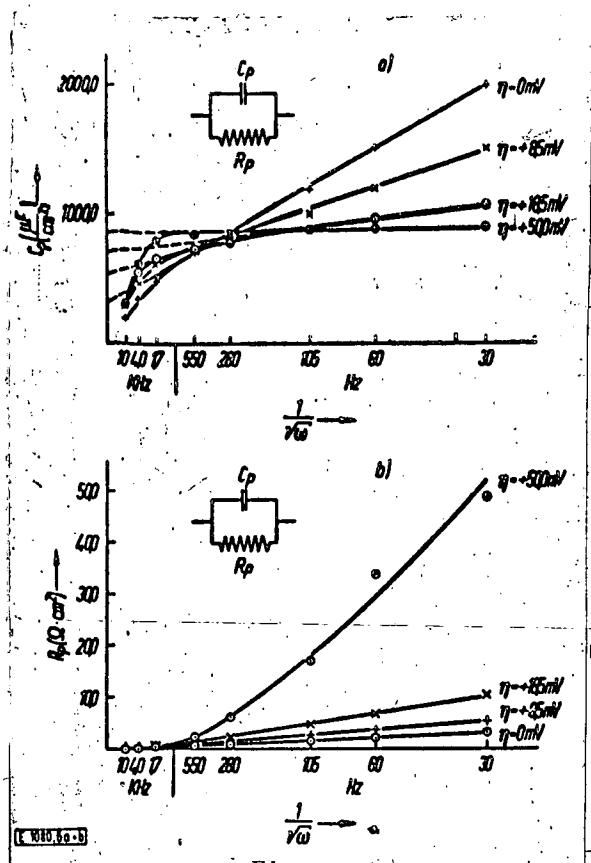

Figure 6

a) Fequency Dependence of C_p at Various Over Voltages in the Potential Range $+50mV \geqslant \eta \geqslant 0$.

b) Frequency Dependence of R_p at Various Over Voltages in the Potential Range $+50mV \geqslant \eta \geqslant 0$.

Tables 3 and 4 compare the C_p and R_p values, calculated according to equations (11,12), with those found experimentaly. Here the magnitude $(2F^2 \cdot c_{H_2})/RT\sqrt{2D}$ determined form the slope of the C_p - $(1)/\sqrt{\omega}$ lines, C_2 from the ordinate section and R from the $(1)/R_p$ value corrected for formula (17) at 20kHz. Table 3 also shows good agreement between the experimental and the calculated C_p values[4]. Somewhat larger deviations were found (cf. Table 4) for the resistance-component R_p.

From the test results mentioned so far, conclusions can be drawn about the degree of coverage of the electrode with adsorbed atomic or molecular hydrogen in the potential range $\eta > 0$. The adsorption capacity C_2, determined in the potential range $\eta >$ + 50mV from the C_p value at 30Hz and in the over voltage range $-10.5mV < \eta \leqslant +50mV$ from the ordinate section obtained by linear extrapolation of the C_p - $1/\sqrt{\omega}$ curves after subtracting the double layer capacity C_D, is ploted in Figure 7 against the overvoltage (broken curve). Thus, in counterdistinction to Figure 3a, Figure 7 eliminates the effect of the H_2 molecule diffusion (cf. also Eucken and Weblus [13]). The fact that C_2 drops from +100mV as potential drops and tends practically toward zero at -10.5mV shows that the member referring to the adsorbed molecular hydrogen $-2Fk\,(dc_{H_2})/d\eta_k$ in equation (9), as opposed to the part conditioned by the atomic adsorbed hydrogen $-F \cdot (dc_H)/d\eta_k$ on smooth platinum electrodes, can be disregarded [6].

[4] [20] Found no agreement between the values produced by Kruger's theory [10] and their measurements, and explained the deviations as caused by the effect of the electrochemical mechanism.

TABLE 3: COMPARISON OF THE C_p VALUES CALCULATED ACCORDING TO EQUATION (11) WITH THE VALUES MEASURED AT OVER VOLTAGES +18.5mV, +8.5mV and OmV

η / $\frac{C_s}{2F^2 \cdot c_H \sqrt{2D}}$ / $\frac{RT}{F}$ / ν (Hz)	+ 18,5 mV 584 µF/cm² $4{,}95 \cdot 10^{-8}\ \Omega^{-2}\,cm^{-2}\,sec^{1/2}$ 0,0322 Ω · cm²		+ 8,5 mV 464 µF/cm² $1{,}33 \cdot 10^{-8}\ \Omega^{-2}\,cm^{-2}\,sec^{1/2}$ 0,0317 Ω · cm²		0 246 µF/cm² $2{,}31 \cdot 10^{-8}\ \Omega^{-2}\,cm^{-2}\,sec^{1/2}$ 0,0317 Ω · cm²	
	C_p Calculated	C_p Measured	C_p Calculated	C_p Measured	C_p Calculated	C_p Measured
10000	304 µF/cm²	322 µF/cm²	300 µF/cm²	280 µF/cm²	255 µF/cm²	197 µF/cm²
4000	570 µF/cm²	560 µF/cm²	485 µF/cm²	480 µF/cm²	365 µF/cm²	351 µF/cm²
1700	704 µF/cm²	676 µF/cm²	597 µF/cm²	610 µF/cm²	467 µF/cm²	493 µF/cm²
550	775 µF/cm²	740 µF/cm²	725 µF/cm²	725 µF/cm²	656 µF/cm²	713 µF/cm²
280	815 µF/cm²	785 µF/cm²	825 µF/cm²	855 µF/cm²	825 µF/cm²	859 µF/cm²
105	895 µF/cm²	891 µF/cm²	1030 µF/cm²	1005 µF/cm²	1181 µF/cm²	1195 µF/cm²
60	965 µF/cm²	969 µF/cm²	1210 µF/cm²	1200 µF/cm²	1480 µF/cm²	1515 µF/cm²
30	1070 µF/cm²	1070 µF/cm²	1510 µF/cm²	1510 µF/cm²	2000 µF/cm²	2000 µF/cm²

TABLE 4: COMPARISON OF THE R_p VALUES CALCULATED ACCORDING TO EQUATION (12) WITH THE VALUES MEASURED AT OVER VOLTAGES +18.5mV, +8.5mV and OmV

η / ν (Hz)	+ 18,5 mV		+ 8,5 mV		0	
	R_p Calculated	R_p Measured	R_p Calculated	R_p Measured	R_p Calculated	R_p Measured
10000	0,049 Ω · cm²	0,0431 Ω · cm²	0,0611 Ω · cm²	0,0435 Ω · cm²	0,0874 Ω · cm²	0,063 Ω · cm²
4000	0,130 Ω · cm²	0,118 Ω · cm²	0,160 Ω · cm²	0,120 Ω · cm²	0,187 Ω · cm²	0,131 Ω · cm²
1700	0,459 Ω · cm²	0,366 Ω · cm²	0,416 Ω · cm²	0,292 Ω · cm²	0,344 Ω · cm²	0,267 Ω · cm²
550	1,97 Ω · cm²	1,38 Ω · cm²	1,07 Ω · cm²	0,96 Ω · cm²	0,697 Ω · cm²	0,630 Ω · cm²
280	3,76 Ω · cm²	2,41 Ω · cm²	1,72 Ω · cm²	1,33 Ω · cm²	1,00 Ω · cm²	0,972 Ω · cm²
105	5,90 Ω · cm²	4,86 Ω · cm²	2,85 Ω · cm²	2,72 Ω · cm²	1,71 Ω · cm²	1,68 Ω · cm²
60	10,1 Ω · cm²	6,75 Ω · cm²	3,80 Ω · cm²	3,82 Ω · cm²	2,21 Ω · cm²	2,26 Ω · cm²
30	14,5 Ω · cm²	10,3 Ω · cm²	5,42 Ω · cm²	5,40 Ω · cm²	3,16 Ω · cm²	3,29 Ω · cm²

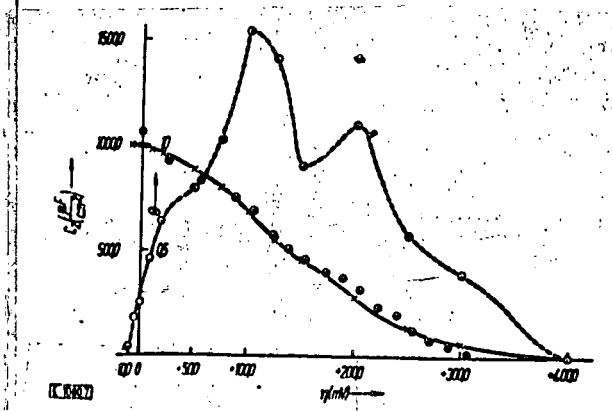

Figure 7

Potential Dependence of the Adsorption Capacity C_2(----) and of the Degree of Coverage Θ^2(× = Θ computed from $\int C_2 d\eta_k$; o = Θ) from Charging Curves according to Voelkl)

This is because otherwise C_2, at least after reaching complete atomic covering (i.e., $(dc_H)/d\eta_k \approx 0$) would have to increase considerably, since C_{H_2} and thus $-2F \cdot k \cdot (dc_{H_2})/d\eta_k$ would have to increase considerably as over voltage drop[5]. If the $C_2 - \eta_k$ curve according to Eucken and Weblus [12] is graphically integrated, we get C_H as a function of η_k (solid curve in Figure 7). Since C_H tends to saturation $C_{H\,max}$, the degree of

[5] Such an increase of C_2 in the over voltage range $\eta < 0$ has actually been observed on platinum-plated platinum with a decrease in n.

covering $\Theta = (C_H)/c_{H\ max}$ was chosen in the ordinate in Figure 7. The integrated curve was standardized in such a way that the value 1 was assigned to the maximum degree of coverage bending clearly toward the limiting value as early as η = 10.5 mV. If we compare this curve with the one from Voelkl [16] by means of charging curves, thus according to the curve of coverage obtained by a completely independent and different method (marked by ⊕ points in Figure 7), we reach a very good agreement. In this way our assumptions about the covering of the electrode with atomic hydrogen is best confirmed. Figure 8 compares the coverage curve (solid diamond ⊕) found experimentally in this work and also independently in the work Voelkl with the coverage curves theoretically computed for the Θ_o values (0.99, 0.95, 0.90) on the basis Langmuir isotherms according to equation (18).

$$\eta = \frac{RT}{2F} \cdot \ln \frac{c_{H_2}}{_0c_{H_2}} = \frac{RT}{F} \ln \frac{1-\Theta}{\Theta} \frac{\Theta_0}{1-\Theta_0} \qquad (18)$$

As is seen, the curves occulated drop much faster with increasing potential then does the coverage curve experimentally determined. The marked maxima of the $C_2 - \eta_k$ and $1/R_p - \eta_k$ curves (Figure 3b) agree with this finding in such a way as to show that there are not only one, but a number of types of atomic hydrogen adsorption on active platinum electrodes and that therefore the coverage curve found experimentally comes into existance through the overlapping of several discrete Langmuir isotherms (cf. also Eucken and Weblus [12]). If we assume not only several (discrete heterogeneities, but very small different kinds of H adsorption centers (continuous heterogeneity), to which various Langmuir isotherms with different coefficients apply, the result is the Temkin isotherm [21] based on a definate distribution. This isotherm, from its derived linear $\Theta - \eta_k$ relationship, represents a far reaching approach to the experimental coverage curve in the potential $+50mV < \eta < +300mV$, because in it the clear maxima of the $C_2 - \eta_k$ curve appears only weakly because of the equalizing effect of integration.

Figure 7 shows that with η = +50mV about 80% of the electrode surface is still covered with atomic hydrogen, although the surface is practically free of molecular hydrogen. The spliting of the H_2 molecules into H atoms also takes place on a far wider surface, uninhibited in comparison with H_2 diffusion.

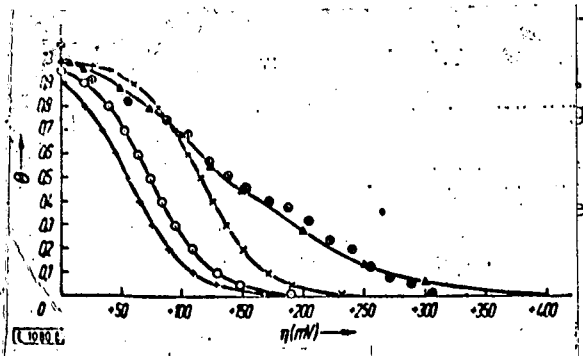

Figure 8

Comparison of the Expermentally Found Coverage Curves (● - Θ according to Voelkl, ▲ = Θ computed from $\int C_2 dn_k$) with Langmuir isotherms for Θ_o = 0.9 (+), Θ_o = 0.95 (⊙) and Θ_o = 0.99 (×).

With the measurements carried out in the area of negative over voltage, a constant direct current was superposed instead of the potential (cf. section 1). The representation of the impedance measurements is applied in series here because of the constantly receding effect of $C_2 + C_D$. Here we first investigated to see how strongly the influence of the couble layer impedance could make itself felt in the most unfavorable case, i.e., if the expected drop in the double layer capacity (cf. P. Dolan and B. Ershler [11] is disregarded with decreasing over voltage. It was shown that the R_s and $(1)/\omega C_s$ differ only slightly with and without double layer correction. For this reason it was superfluous to plot the corrected values in the corresponding figures. In Figure 9 the R_s and $(1)/\omega C_2$ values, measured at several negative over voltages, are ploted as a function of $(1)/\sqrt{\omega}$. It is seen that, as a consequence of the still considerable effect of C_2, the imaginary component $(1)/\omega C_s$ at zero potential is still greater than the real component R_s, and therefore the curves continue to be somewhat curved. At η = -10.5mV, both resistance components then coinside in a straight line going through the coordinate origin, from which it can be deduced that C_2 here, as a result of the still almost complete coverage of the surface with H atoms, has become very small, and therefore the H_2 diffusion is almost exclusively decisive of concentration for the impedance. Finally for η < - 10.5mV becomes $(1)/\omega C_s$, by an amount dependent upon frequency, so that the /45
two components appear in the shape of two parallel straight lines. If C_2 = 0, then for R_2 and $(1)/\omega C_2$ in agreement with equation (10):

$$R_s = r + \frac{RT}{4F^2}\frac{1}{c_{H_2}}\frac{1}{\sqrt{2D\omega}} \qquad (19)$$

$$\frac{1}{\omega C_s} = \frac{RT}{4F^2}\frac{1}{c_{H_2}}\frac{1}{\sqrt{2D\omega}}. \qquad (20)$$

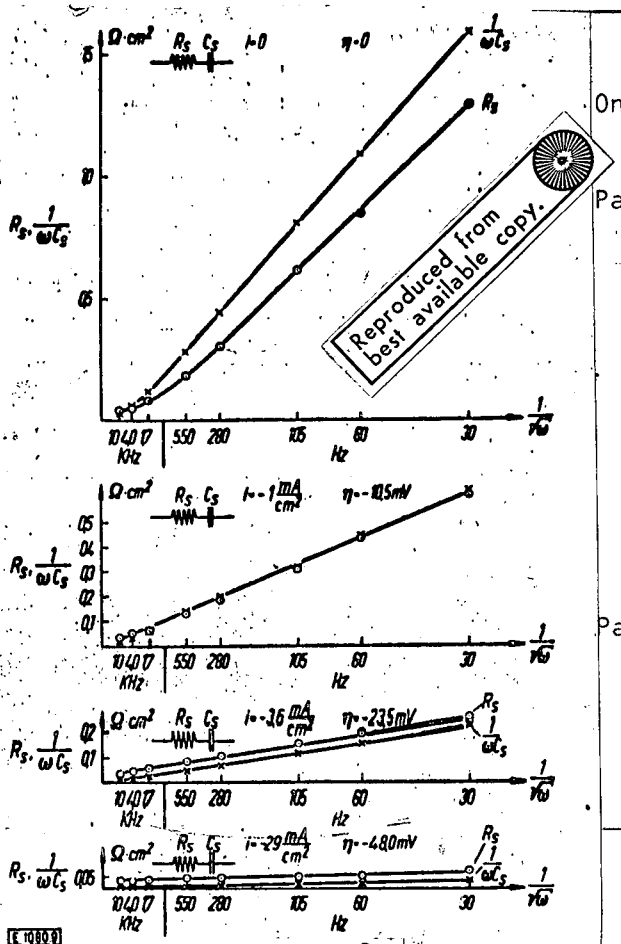

Figure 9

Frequence Dependency of the Resistant and Capacitive Components of the Alternating Current Resistance in Series at Several Negative Over Voltage Values (⊙ = Resistant Component R_s, × = Capacitive $(1)/\omega C_2$)

Similar expressions for the alternating current resistance in diffusion and discharge obstruction have already been given in general for redox systems by several authors [22,23,8]. In Figure 10 all of the $(1)/\omega C_2$ - $(1)/\sqrt{\omega}$ straight lines, measured in the potential range $\eta \leq -10.5$mV, are compared. According to equation (20) there slopes are inversely proportional to the corresponding H_2 concentration. For the over voltage range +50mV > η > - 10.5mV, the $(1)/\sqrt{\omega}$ curves and C_{H_2} can be calculated from equation (13) from the drop in the straight portion at low frequencies. With the help of the Nernst equation[6], which can be contrasted with those measured directly (cf. Table 5), can be gotten for the molecular hydrogen from the H_2 concentrations determined in the above manner.

The fine agreement between the calculated and measured over voltage at lower current densities confirms the fact that practically only diffusion over voltage takes place in this range. In counterdistinction to the measured over voltage, the calculated over voltage with greater cathodic current densities approaches a limiting value at about

[6] If for this purpose the quotients are found form the inclination of two $(1)/C_2$ - $(1)/\sqrt{\omega}$ - $(1)/\sqrt{\omega}$ straight lines, the additional coefficient of inclination $(RT)/4F^2$ $(1)/\sqrt{2D}$ and $(2F^2)/RT\sqrt{2D})$ is simplified.

-70.0mV (cf.Figure 11). This shows that from a certain cathodic current density on the H_2 concentration on the electrode surface no longer increases because of the removal of the hydrogen by blister formation. This demonstrates that the limiting value of diffusion over voltage, found earlier on active palladium electrodes [24], also applies to active platinum electrodes.

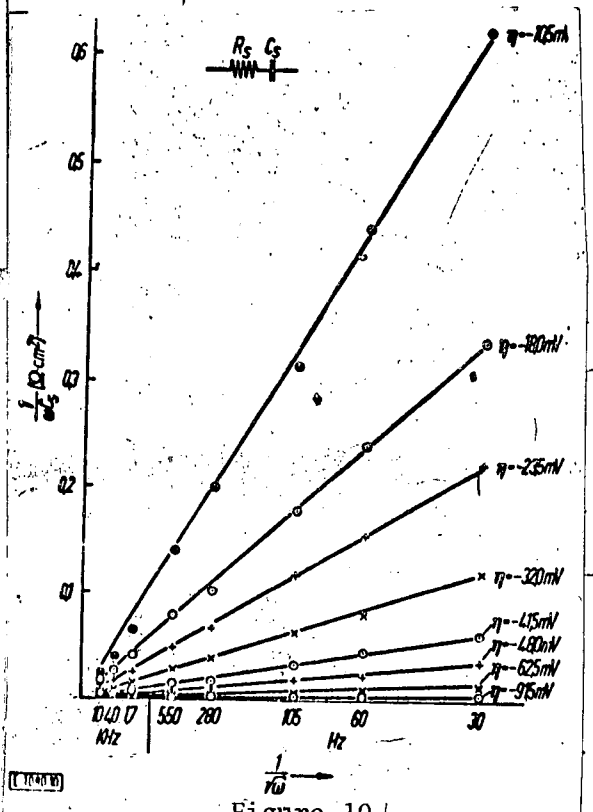

Figure 10 / Comparison of the $(1)/\omega C_2$ - $(1)/\sqrt{\omega}$ Straight Lines Measured in the Potential Range $\eta \leqslant$ - 10.5mV

The difference $\Delta\eta = \eta - \eta_d$ between the measured and calculated over voltage, likewise shown in Figure 11, turns out to be approximately proportional to the current density. The slope of the $\Delta\eta$-i straight lines has a value of 0.0725Ω·cm². If the Ohm resistance of the electrolyte solution, determined quite exactly in another way with 0.0475Ω·cm², the remainder of 0.025Ω·cm² is practically identical to the $(d\eta/di)$ value of 0.027Ω·cm² found in alternating current measurements for $\eta <$ - 62.5mV. Thus in the difference $\Delta\eta$, in addition to the resistance over voltage η_Ω always determinable, there is also a determinable portion of mean over voltage which, as a result of the high exchange current density of about 0.9 A/cm² in the cathodic over voltage range investigated, is still linearly dependent on the current density. Finally R_p, measured at 20kHz, is introduced in Table 6 for the total potential range investigated with the various η values. R_p (20kHz) approximately represents, as is clear from Figure 5b, the discharge resistance $r = (d\eta/di)$. The table shows that form +200mV Rp (20kHz) increases intensively with increasing positive over voltage. This increase has already been explained by Dolan and Ersher [11] as caused by the decreasing coverage of the electrode surface with adsorbed H atoms as the over voltage rises. However, in the range $\eta \leq$ +200mV, R_p (20kHz) remains approximately constant, while it should

pass through a minimum, on the assumption that the H^+ ion discharge is possible only at vacant points of the surface [25], and then increase again. This indicates that the discharge of the H^+ ions can also take place at occupied points. In order to show how the discharge resistance are in connection with a direct current flux makes itself felt along with the diffusion resistance $(d\eta_d)/di$ [26] as a function of potential, the numerical values of the quotient $(r)/d\eta_d/di$ had been introduced in Table 7. For calculation of $(d\eta_d)/di$ equation (21)

$$\frac{d\eta_d}{di} = \frac{RT}{2F} \frac{1}{1 - i/i_{gr}} \cdot \frac{1}{i_{gr}} \qquad (21)$$

was used with the experimental value of 730 μ A/cm² for $i_{measured}$. As can be seen from the table, the discharge obstruction relative to diffusion becomes clearer and clearer as the cathodic overvoltage increases. A similar comparison of r with the value $(d\eta)/di$, found from the inclination of the current voltage curve, corresponding to our $(d\eta_d)/di$, was carried out by Dolan, Ershler and Frumkin [27] on platinum in 1n-HCl with $\eta = 0$. For the quotient $(r)/(d\eta)/di$, these authors found the value $4.55 \cdot 10^{-2}$, while we found $1.76 \cdot 10^{-3}$ at $\eta = 0$. Thus a relatively essentially smaller passage inhibition occured on our electrodes. With our measurements an exchange current density of about 0.9A/cm² in the range $\eta < +200$mV can be computed from R_p (20kHz). At the moment we are still not able to distribute this numerical value into various discharge mechanisms according to Volmer [28] and Horiuti [29, 30].

A few tests were also carried out on platinum plated platinum. Because of the extraordinary small resistance values, we had to limit our measurement to the low frequency range ($\nu \leqslant 280$ Hz). The tests led to the result that, in counterdistinction to smooth platinum, the impedance was determined at only in the range of positive but also of negative over voltages, predominately through a large adsorption capacity which even increased somewhat with a drop in potential. In accord with equation (9), it seems that considerable molecular hydrogen, in addition to the atomic hydrogen in the cathode over voltage range, was also adsorbed as a result of the much greater actual electrode in comparison to the smooth platinum. The diffusion of the molecular hydrogen does not become very noticable here, because only the much smaller geometric surface is suitable for it.

TABLE 5: DIFFUSION OVER VOLTAGE VALUES, CALCULATED ACCORDING TO EQUATION (20) AND (13), AS WELL AS THE NERNSTS EQUATION, FOR MOLECULAR HYDROGEN, COMPARED WITH THE MEASURED OVER VOLTAGE IN THE RANGE $-90\ mV \leqslant \eta \leqslant +50\ mV$.

$i\ mA/cm^2$	+ 0,53	+ 0,33	0	− 0,44	− 1,0	− 2,17	− 3,62	− 7,25	− 14,5	− 29,0	− 72,5	− 145	− 290
η_{meas} (mV)	+ 18,5	+ 8,5	0	− 6,0	− 10,5	− 18,0	− 23,5	− 32,0	− 41,5	− 48,0	− 62,5	− 76,5	− 91,5
η_{calc} (mV)	+ 20,2	+ 7,8	+ 0,8	− 5,75	− 10,5	− 18,3	− 23,2	− 31,3	− 39,8	− 46,5	− 58,0	− 65,5	− 70,2

Note: Commas indicate decimal points.

TABLE 6: DEPENDENCE OF THE R_p -(20kHz) VALUES ON THE OVER VOLTAGE

η (mV)	− 91,5	− 76,5	− 62,5	− 48,0	− 41,5	− 32,0	− 23,5	− 18,0	− 10,5	− 6,0	0	+ 8,5
$R_p\ \Omega \cdot cm^2 \cdot 10^3$	2,70	2,69	2,83	3,04	2,97	2,94	3,10	2,96	3,00	2,67	2,97	2,97
η (mV)	+ 18,5	+ 50,0	+ 75,0	+ 100,0	+ 125,0	+ 150,0	+ 200,0	+ 250,0	+ 300,0	+ 400,0		
$R_p\ \Omega \cdot cm^2 \cdot 10^3$	3,00	3,04	2,99	2,94	2,88	3,05	2,87	5,10	9,80	47,6		

Note: Commas indicate decimal points.

TABLE 7: QUOTIENT FROM THE DISCHARGE RESISTANCE r AND THE TANGENT $(d\eta_d)/di$ OF THE CURRENT VOLTAGE CURVE AS A FUNCTION OF THE PONTENTIAL IN THE RANGE $-50mV < \eta < +50mV$; ARE RESULTS FROM R_p(20kHz) AND $(d\eta_d)/di$ FROM EQUATION (21) WITH $i_{gr} = 730\mu A/cm^2$

η (mV)	+ 18,5	+ 8,5	0	− 6,0	− 10,5	− 18,0	− 23,5	− 32,0	− 41,5	− 48,0
$\frac{r}{\frac{d\eta_d}{di}} \cdot 10^6$	4,9	9,6	17,6	25,4	42,5	70,0	110,0	191,0	368,0	735,0

Note: Commas indicate decimal points.

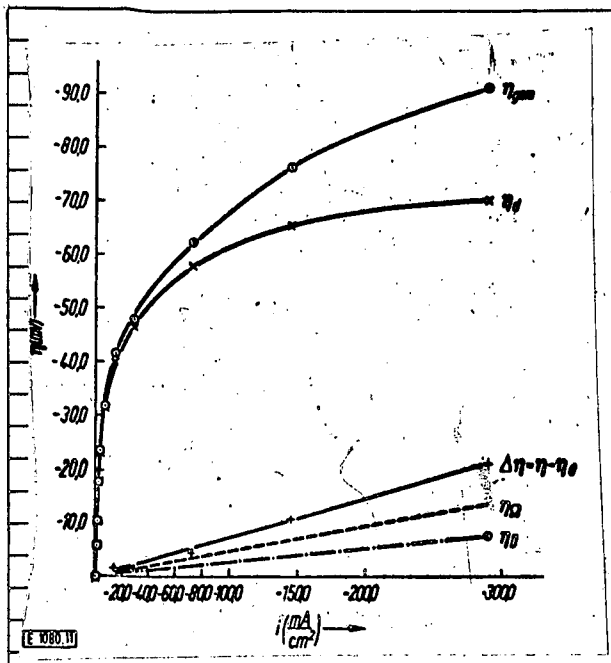

Figure 11. Current Voltage Curves in the Potential Range $\eta < 0$. $\odot = \eta_{calculated} = \eta_d$; $+ = \Delta\Omega = \eta - \eta_d$; Resistance overvoltage $\eta\Omega$ (----), Mean overvoltage η_d (-·-·-·).

4. Summary

1. A description is given of the test apparatus with which measurements of the alternating current resistance R of direct current polarized and activated platinum electrodes were carried out in 8n-H_2SO_4 rinsing.

2. It is clear from the frequency dependence of the alternating current resistance that R in the potential range +50 mV $\leqslant \eta \leqslant$ +400 mV is essentially conditioned by the adsorption capacity C_2, affected by a certain loss angle, and the passage resistance r associated with it in series. For $\eta \leqslant$ +50 mV the diffusion of the H_2 molecules also appears. In correspondence with this finding is the fact that the diffusion limiting current is practically reached with $\eta \geqslant$ +50 mV, and thus the H_2 concentration disappears.

3. The potential dependence of C_2 shows that the covering of the electrode surface with adsorbed atomic hydrogen at $\eta \leqslant$ -10.5 mV is already tending toward saturation. The covering curve, obtained by graphic integration of C_2 (ηk) across ηk, agrees very well with what was found by Voelkl [16] in another way.

4. In the potential range $\eta \leqslant$ -10.5 mV, the alternating current resistance is determined only by the H_2 diffusion and the H^+ ion discharge, since C_2 practically disappears as a consequence of the almost completely obtained

coverage. In counterdistinction to discharge, the influence of diffusion constantly recedes as the overvoltage.

Page One Title

5. The diffusion overvoltage η_d can be computed from the inclination of the $1/\omega C_2 - 1/\sqrt{\omega}$ straight lines in the potential range $\eta \leqslant -10.5$ mV and the $C_p - (1)/\sqrt{\omega}$ lines for $-10.5\ \text{mV} \leqslant \eta \leqslant +50$ mV according to the Nernst equation E form molecular hydrogen. Because of the beginning of blister formation, η_d approaches a limiting value at around $\eta_d = -70$ mV. The difference between the calculated and measured overvoltage is approximately proportional to the current density and can be divided quantitatively into portions of resistance overvoltage η_Ω and passage overvoltage η_d. The estranged current density of the latter amounts to about 0.9 A/cm^2 for cathodic overvoltages.

Cover Page Source

6. The frequency dependence of the resistance components in the total overvoltage area investigated confirms the fact that the H_2 combining equilibrium was practically standardized for the electrodes investigated. In spite of the saturation of the surface with adsorbed atomic hydrogen, no cathodic limiting current appears.

(4'')

7. The potential dependence of the resistance R_p (20 kHz), which represents a measurement for discharge inhibition, shows that the discharge of the H^+ ions takes place with relatively little inhibition not only on free, but also on occupied points of the surface.

This work was carried out with the support of the German Research Association. One of the authors (H. Kammermaier) is grateful to the Battelle Memorial Institute for Germany for granting a research stipend.

NASA

REFERENCES

1. Kammermaier, H., *Dissertation*, Technical University, Munich, 1955.
2. Opitz, G., *Hichfrequenztechn u. Elektroakust*, Vol. 49, p. 52, 1937.
3. Gerischer, H., *Z. Elektrochem. Ber. Bunsenges. physik. Chem.*, Vol. 59, p. 9, 1954.
4. Elmore, W. C. and M. Sands, *Electronics*, New York, p. 99, 1949.
5. Breiter, M., H. Kammermaier and C. A. Knorr, *Z. Elektrochem. Ber. Bunsenges, physik. Chem.*, Vol. 58, p. 702, Figure 2, 1954.
6. De Boer, J. H., "Electron Emissions and Adsorption Phenomena," Leipzig, p. 46, 1937.
7. Grahame, D. C., *J. Electrochem. Soc.*, Vol. 99, p. 370, 1952.
8. Gerischer, H., *Z. physik. Chem.*, Vol. 198, p. 28, 1951; Vol. 201, p. 55, 1952; N. F. p. 278, 1954.
9. Warburg, E., *Ann. Physik*, Vol. 6, p. 125, 1901.
10. Krueger, F., *Z. physik. Chem.*, Vol. 45, p. 1, 1903.
11. Dolin, P. and B. Ershler, *Acta Physiocochim.*, USSR, Vol. 13, p. 747, 1940.
12. Eucken, A. and B. Weblus, *Z. Elektrochem. angew. physik. Chem.*, Vol. 55, p. 114, 1951.
13. Wicke, E. and B. Weblus, *Z. Elektrochem. Ber. Bunsenges, physik. Chem.*, Vol. 56, p. 169, 1952.
14. Breiter, M., C. A. Knorr and R. Meggle, *Z. Elektrochem. Ber. Bunsenges, physik. Chem.*, Vol. 59, p. 153, 1955.
15. Robertson, W., *J. Electrochem. Soc.*, Vol. 10, p. 194, 1953.
16. Breiter, M., C. A. Knorr and W. Voelkl, *Z. Elektrochem. Ber. Bunsenges. physik. Chem.*, Vol. 59, p. 681, 1955.
17. Frumkin, A. and A. Slygin, *Acta physicochim. URSS*, Vol. 3, p. 791, 1935 and and Vol. 4, p. 911, 1936.
18. Ershler, B., *Acta physicochim. URSS*, Vol. 7, p. 327, 1938.
19. Pearson, J. D. and J. V. Butler, *Trans. Faraday Soc.*, Vol. 34, p. 1163, 1938.
20. Frumkin, A., P. Dolan and B. Ershler, *Acta physicochim. URSS*, Vol. 13, p. 793, 1940.
21. Temkin, M., *J. physik. Chem.*, Vol. 15, p. 296, 1941.
22. Randles, E. B., *Discuss. Faraday Soc.*, Vol. 1, p. 11, 1947.
23. Ershler, B., *Discuss. Faraday Soc.*, Vol. 1, p. 269, 1947.
24. Clamroth, R., and C. A. Knorr, *Z. Elektrochem. Ber. Bunsenges. physik. Chem.*, Vol. 57, p. 399, 1953.
25. Breiter, M. and R. Clamroth, *Z. Elektrochem. Ber. Bunsenges. physik. Chem.*, Vol. 58, p. 493, 1954: e.g., equation (46).
26. Gerischer, H., *Z. Elektrochem. angew. physik. Chem.*, Vol. 55, p. 98, 1951.
27. Dolin, P., B. Ershler and A. Frumkin, *Acta physicochim. URSS*, Vol. 13, p. 779, 1940.

28. Volmer, M. and T. Erdey-Gruz, *Z. physik, Chem.*, Vol. 150, p. 203, 1930.
29. Horiuti and G. Okamoto, *Sci. Pap. Inst. physic. chem. Res.*, Tokyo, Vol. 28, p. 231, 1936.
30. Vetter, K. J., *Z. Elcktrochem. Ber. Bunsenges. physi,. Chem.*, Vol. 59, p. 435, 1955.

Page One Title

Cover Page Title

Translated for the National Aeronautics and Space Administration under contract No. NASw-2037 by Techtran Corporation, P. O. Box 729, Glen Burnie, Maryland 21061, translator: Lawrence W. Murphy, Ph.D.

Cover Page Source

(4")

NASA